

Non-equilibrium correlations and entanglement in a semiconductor hybrid circuit-QED system

L. D. Contreras-Pulido,¹ C. Emary,^{2,3} T. Brandes,³ and R. Aguado⁴

¹*Institut für Theoretische Physik, Albert-Einstein Allee 11, Universität Ulm, D-89069 Ulm, Germany*

²*Department of Physics and Mathematics, University of Hull, Kingston-upon-Hull, HU6 7RX, United Kingdom*

³*Institut für Theoretische Physik, Hardenbergstrasse 36, TU Berlin, D-10623 Berlin, Germany*

⁴*Instituto de Ciencia de Materiales de Madrid (ICMM), Consejo Superior de Investigaciones Científicas (CSIC), Sor Juana Inés de la Cruz 3, 28049 Madrid, Spain*

(Dated: May 17, 2022)

We present a theoretical study of a hybrid circuit-QED system composed of two semiconducting charge-qubits confined in a microwave resonator. The qubits are defined in terms of the charge states of two spatially separated double quantum dots (DQDs) which are coupled to the same photon mode in the microwave resonator. We analyze a transport setup where each DQD is attached to electronic reservoirs and biased out-of-equilibrium by a large voltage, and study how electron transport across each DQD is modified by the coupling to the common resonator. In particular, we show that the inelastic current through each DQD reflects an indirect qubit-qubit interaction mediated by off-resonant photons in the microwave resonator. As a result of this interaction, both charge qubits stay entangled in the steady (dissipative) state. Finite shot noise cross-correlations between currents across distant DQDs are another manifestation of this nontrivial steady-state entanglement.

PACS numbers:

I. INTRODUCTION

Recent technological progress has made it possible to coherently couple superconducting qubits to microwave photons on a superconducting chip.¹ This so-called circuit quantum electrodynamics (circuit-QED)² has paved the way to new research directions beyond standard cavity QED systems.^{3–5} Apart from the high degree of tunability in circuit-QED, most of the novelty comes from the fact that the coupling between qubits and microwave photons can reach values well above the ones between natural atoms and photons in optical cavities.⁶

An interesting alternative to the above ideas is to implement hybrid circuit-QED⁷ with qubits defined in semiconducting quantum dots (QDs),^{8–12} as has been experimentally implemented recently.^{13–17} In these hybrid structures, the semiconducting QDs are typically coupled to normal electronic reservoirs such that electronic transport may be used to characterize/modify the properties of the circuit-QED system. This possibility has remained largely unexplored, except for some works analyzing the transport-induced lasing states in the resonator.^{18–21}

In this context, we here analyze how the coupling to a common photon mode generates entanglement between distant charge qubits realized in double quantum dots (DQDs) and how this entanglement manifests in the transport properties of the system. In particular, we present a detailed analysis of how the electron currents across each DQD are modified due to the interaction with the photons in the circuit. The coupling of each DQD to a common microwave resonator generates an indirect coupling between DQDs which gives rise to positive shot noise cross-correlations between *distant* currents across

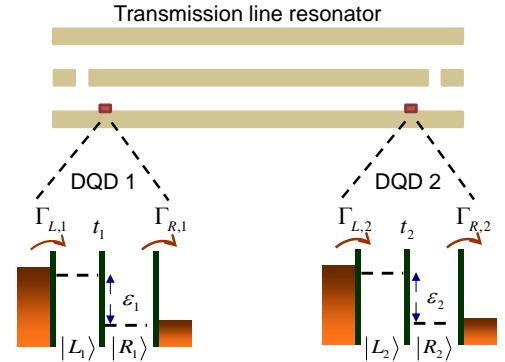


FIG. 1: (Color online) Schematics of the two charge qubits coupled to a transmission line resonator. An excess charge in each double dot (formed by the L_i and the R_i dots) defines the states of the qubit. Both qubits are attached to electronic reservoirs, via the rates $\Gamma_{L,i}$ and $\Gamma_{R,i}$, such that an electrical current pass through them. The qubits are located at the ends of the resonator in order to enhance the coupling with the electromagnetic field.

them. We analyze this physics in terms of an effective model and show that off-resonant photons are responsible for the induced indirect coupling. Moreover, we demonstrate that both charge qubits are entangled in the steady (dissipative) state due to this cavity-induced coupling.

The paper is organized as follows. In section II we describe the model for two double quantum dots coupled to a microwave resonator as well as the master equation that governs the dynamics of this open quantum system. In section III we discuss the stationary transport prop-

erties (mean value of the current and shot noise) of the system. This section is divided in two parts. The first part (subsection III A) reviews the case of a single double quantum dot. We then turn to the analysis of the two double quantum dot system (subsection III B) by calculating also shot-noise cross-correlations between distant currents across each double quantum dot. In Section IV we focus on the generation of qubit-qubit entanglement induced by the common coupling to a microwave photon mode, and compare it with the results obtained for the cross-correlations in the previous section. In particular, we present a detailed analysis of steady-state Bell state occupations and demonstrate that indeed cross-correlations between distant currents constitute an indicator of non-local qubit-qubit entanglement. In section V we extend our study to the case of asymmetric couplings between each double quantum dot and the microwave resonator. Our conclusions are presented in section VI.

II. MODEL

We consider the coupling of the charge states of two uncoupled semiconductor DQDs to an electromagnetic resonator with a high Q -factor, as for instance the superconducting transmission line described in the recent experiments of Ref. 15. We assume that the DQDs are placed at the ends of the resonator, as schematically depicted in figure 1. In the following, we consider that the charging energy on each DQD is the largest energy scale of the problem such that, for each individual DQD, an excess electron defines the two states of a charge qubit, $|L_i\rangle$ and $|R_i\rangle$ ($i = 1, 2$), see e.g. Ref. 22. In this basis, the Hamiltonian describing the DQDs reads

$$H_{el} = \sum_i \left(\frac{1}{2} \varepsilon_i \sigma_z^i + t_i \sigma_x^i \right) \quad (1)$$

where the energy detuning in each DQD is given by ε_i , t_i is the tunneling coupling between dots of the i -th DQD and σ_j is the j -th Pauli matrix acting on the charge basis of each qubit, namely $\sigma_z^i \equiv |L_i\rangle\langle L_i| - |R_i\rangle\langle R_i|$ and $\sigma_x^i \equiv |L_i\rangle\langle R_i| + |R_i\rangle\langle L_i|$.

The transmission line resonator is modeled as a quantum harmonic oscillator $H_{res} = \hbar\omega_r a^\dagger a$, where a^\dagger (a) is the creation (annihilation) operator of photons in the resonator with frequency ω_r . The charge states of each qubit are coupled to the same mode of the resonator, such that the coupling term reads

$$H_{e-res} = \sum_i \hbar g_i \sigma_z^i (a^\dagger + a). \quad (2)$$

Experimentally, typical photon frequency values range from 1 to 10 GHz, whereas couplings strengths $g \sim 10$ -30 MHz have been reported for a single DQD coupled to a microwave resonator.^{15,16}

Finally, we consider that each DQD ($i=1,2$) is coupled to electronic reservoirs described by the Hamiltonian

$$H_{leads} = \sum_i \sum_k \{ \varepsilon_{k,i}^L c_{kL,i}^\dagger c_{kL,i} + \varepsilon_{k,i}^R c_{kR,i}^\dagger c_{kR,i} \} \quad (3)$$

in which $c_{k\beta,i}^\dagger$ ($c_{k\beta,i}$) is the creation (annihilation) operator of electrons in the left/right contact, $\beta \in L, R$, with energy $\varepsilon_{k,i}^\beta$. The coupling of each DQD to the leads reads:

$$H_{int} = \sum_i \sum_k \{ V_{k,i}^L c_{kL,i}^\dagger d_{L,i} + h.c. + L \rightarrow R \} \quad (4)$$

where $d_{L/R,i}$ ($d_{L/R,i}^\dagger$) creates (annihilates) an electron in the left/right QD of each DQD, and $V_{k,i}^\beta$ are the tunneling matrix elements. Due to this coupling to the reservoirs, situations in which either of the two DQDs (or both) are empty need to be considered and hence the Hilbert space in the charge sector is spanned by the states $|\alpha_1, \alpha_2\rangle$, with $\alpha = L, R, 0$. This transport model can be easily extended to a system consisting of several qubits, see e.g. Ref. 23, and is the single-mode version of previous studies focusing on bath-mediated interactions.²⁴

The total Hamiltonian of the system is given by $H_{tot} = H_{el} + H_{res} + H_{e-res} + H_{leads} + H_{int}$. The dynamics of the resonator and the DQDs is described by the master equation for the reduced density matrix $\rho(t)$ obtained after tracing out the reservoirs degrees of freedom and applying a Born-Markov approximation with respect to the Hamiltonian H_{int} .^{25,26} In the Schrödinger picture the master equation reads $\dot{\rho}(t) = \mathcal{L}\rho$ with the Liouvillian:

$$\begin{aligned} \mathcal{L}\rho = & -i[H_{el} + H_{res} + H_{e-res}, \rho(t)] \\ & - \sum_i \frac{\Gamma_i^L}{2} \left(d_{L,i} d_{L,i}^\dagger \rho(t) - 2d_{L,i}^\dagger \rho(t) d_{L,i} + \rho(t) d_{L,i} d_{L,i}^\dagger \right) \\ & - \sum_i \frac{\Gamma_i^R}{2} \left(d_{R,i}^\dagger d_{R,i} \rho(t) - 2d_{R,i} \rho(t) d_{R,i}^\dagger + \rho(t) d_{R,i}^\dagger d_{R,i} \right) \\ & - \frac{\kappa}{2} (a \rho(t) a^\dagger - 2a^\dagger a \rho(t) + \rho(t) a^\dagger a) \end{aligned} \quad (5)$$

with the tunneling rates to reservoirs $\Gamma_i^\beta = 2\pi \sum_{k,i} |V_{k,i}^\beta|^2 \delta(\varepsilon_{i,\beta} - \varepsilon_{k,i,\beta})$ and where we considered the limit of infinite source-drain voltage, $\mu_L \rightarrow \infty$ and $\mu_R \rightarrow -\infty$ (such that the Fermi functions in the reservoirs become $f_L = 1$ and $f_R = 0$). In this limit, the Born-Markov approximation with respect to the coupling to reservoirs is essentially exact and, more importantly, the physics no longer depends on the temperature of the electronic reservoirs.^{27,28} The damping of the bosonic system at zero temperature, with rate κ ,²⁹ has also been taken into account by including the last Lindblad term in equation (5).

We are interested on the generation of qubit-qubit entanglement and on the transport properties in the stationary state, ρ^{stat} . This can be obtained from equation (5) as $\dot{\rho}(t) = \mathcal{L}\rho^{\text{stat}} = 0$ such that the Liouvil-

lian \mathcal{L} has a zero eigenvalue with right eigenvector denoted as $|0\rangle\rangle = \rho^{\text{stat}}$. The corresponding left eigenvector is $|\tilde{0}\rangle\rangle$ such that the probability conservation reads $\langle\langle\tilde{0}|0\rangle\rangle = \text{Tr}[\hat{1}\rho^{\text{stat}}] = 1$. Using this language, the average of any operator \hat{A} acting on the qubits-resonator system reads $\langle\langle\hat{A}\rangle\rangle = \text{Tr}[\hat{A}\rho^{\text{stat}}] = \langle\langle\tilde{0}|\hat{A}|0\rangle\rangle = \langle\langle\hat{A}\rangle\rangle$.

The set of equations for the elements of the density matrix $\rho_{nm}(t)$, in the basis given by the direct product of the electronic states and the oscillator Fock states $|\alpha_1, \alpha_2\rangle \otimes |n\rangle$ (with $n = 0, 1, 2, \dots$), is solved numerically by truncating up to a maximum number of photon states $n = N_{\text{max}}$. We take the order of magnitude of the parameters from the recent experiments reporting circuit-QED devices with semiconducting QDs.^{15,16} Even though we focus here on this moderate coupling regime $g/\omega_r \sim 10^{-2}$, we note in passing that our numerical scheme allows in principle to include stronger couplings, such as the ones already achieved in circuit-QED architectures with superconducting qubits.^{6,30}

III. STATIONARY TRANSPORT PROPERTIES: CURRENT, SHOT NOISE AND CURRENT CORRELATIONS

We expect that the indirect, non-local two-qubit interaction induced by the coupling to a common resonator mode can be revealed in transport through either DQD. As previously mentioned, we restrict ourselves to the Coulomb blockade regime in the infinite bias voltage limit.

In this case of unidirectional transport, the total current passing through the DQD i is described by the operator $\mathcal{I}_i = e\Gamma_{R,i}d_{R,i}\rho d_{R,i}^\dagger$, and the corresponding steady-state expectation value reads $I_i = \langle\langle\tilde{0}|\mathcal{I}_i|0\rangle\rangle = \text{Tr}[\mathcal{I}_i\rho^{\text{stat}}]$.

We also analyze the non-equilibrium quantum noise, resulting from the temporal fluctuations of the current, by means of the current-current correlation function $\langle\langle\Delta I_i(\tau), \Delta I_j(0)\rangle\rangle$, with $\Delta I_i(t) = I_i(t) - \langle I_i \rangle$. The Fourier transform of such correlation function defines the power spectral density of shot noise:

$$S_{ij}(\omega) = 2 \int_{-\infty}^{\infty} d\tau e^{i\omega\tau} \langle\langle\{\Delta I_i(\tau), \Delta I_j(0)\}\rangle\rangle \quad (6)$$

It has been shown that this finite-frequency power spectral density contains a great deal of information about internal dynamics of the system.³¹ Nevertheless, we here restrict the analysis to zero frequencies for simplicity. In particular we focus on the cross-correlations which, as we shall show, exhibit features related with the qubit-qubit effective interaction induced by the common coupling to the resonator. Additional interest in studying shot noise and cross-correlations reside in theoretical proposals which make use of current correlations to study and detect entanglement in mesoscopic systems.³²⁻³⁹

In practice, the shot noise at zero-frequency is calculated in terms of the inverse of the part of the Liouvillian that is non-singular at zero-frequency (or pseudo-inverse), $R = \mathcal{Q}\mathcal{L}^{-1}\mathcal{Q}$ (with $\mathcal{Q} = 1 - |0\rangle\rangle\langle\langle\tilde{0}|$), see e.g. Refs. 40-42. The diagonal part of the noise reads $S_{ii}(0) = 2(\langle\langle\mathcal{I}_i\rangle\rangle - 2\langle\langle\mathcal{I}_i R \mathcal{I}_i\rangle\rangle)$, with $i = 1, 2$, whereas the off-diagonal noise cross-correlations read $S_{12}(0) = S_{21}(0) = -2(\langle\langle\mathcal{I}_1 R \mathcal{I}_2\rangle\rangle + \langle\langle\mathcal{I}_2 R \mathcal{I}_1\rangle\rangle)$. Note that any finite off-diagonal noise in this setup indicates correlations between *distant* currents across each DQD.

In what follows we present our noise results in the form of Fano factors, defined as $F_{ij} = S_{ij}(0)/(2e\sqrt{I_i I_j})$, which quantifies deviations from the Poissonian noise originated by uncorrelated carriers. In particular, super-Poissonian noise ($F > 1$) is related to a bunching behavior, of the carriers whereas sub-Poissonian noise ($F < 1$) signals anti-bunching.⁴³

A. A single DQD coupled to the resonator

To set the stage for our study, we begin by analyzing the case of a single DQD coupled to the cavity. The physics here is that of inelastic transport through a two-level system, a problem which has received a lot of attention in various contexts.^{28,44-52} In the frame of circuit-QED with semiconducting qubits, the problem has been theoretically studied in Refs. 19 and 20 mainly with focus on lasing.

In figure 2a) we show the current in the DQD as a function of its level detuning ε_1 (all the parameters are expressed in units of the resonator frequency ω_r). As expected, there is an elastic peak in the current around $\varepsilon_1 = 0$ which corresponds to resonant tunneling across the DQD. Here, the electronic transport occurs by the tunnel coupling with the reservoirs, which we assumed to be the same for both leads $\Gamma_{L,1} = \Gamma_{R,1}$. The height and width of the elastic peak is in agreement with the well known analytical expression for the current through a DQD.^{27,53} For finite detuning (i.e., with the electronic levels of the DQD far from resonance) the current is suppressed except at values of ε_1 corresponding to a resonance condition at which the frequency of the qubit $\Omega_1 \equiv \sqrt{\varepsilon_1^2 + 4t_1^2}$ equals the frequency of the resonator ω_r . This feature corresponds to inelastic processes in which the tunneling of an electron between the left and right dots of the qubit excites the state of the resonator. This behavior is in qualitative agreement with the theoretical results of Jin *et al.*,¹⁹ who studied lasing in a DQD-based circuit-QED system (the main idea being that transport of electrons through the artificial two-level system can lead to a population inversion and induce a lasing state in the microwave resonator). Although we are not interested on analyzing the specific lasing conditions, the underlying mechanism giving rise to the inelastic peak of the current is the same.⁵⁴ Finally, we mention in passing that the physics is also similar to one of spontaneous emission of a DQD coupled to a bath of phonons, demon-

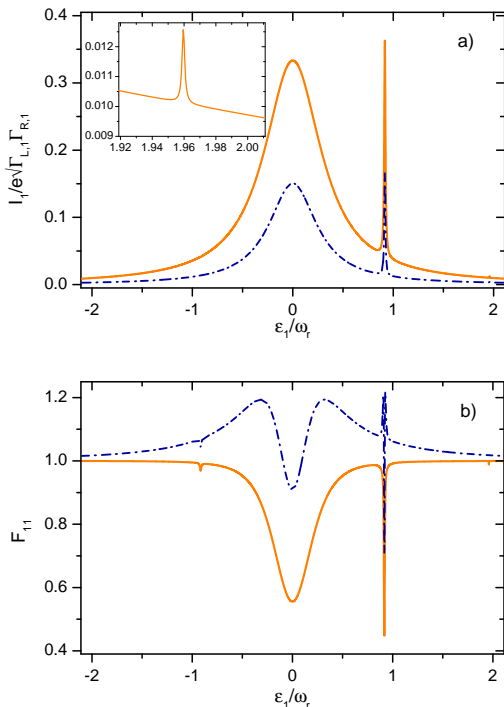


FIG. 2: (Color online) Results for a) stationary current and b) Fano factor for a single-qubit coupled to a transmission line resonator. The solid line corresponds to equal tunneling rates to the reservoirs ($\Gamma_{L,1} = \Gamma_{R,1} = 10^{-3}$) and the dashed line to asymmetric rates ($\Gamma_{L,1} = 0.01, \Gamma_{R,1} = 10^{-3}$). Note that the inelastic peaks appear at values of ϵ_1 corresponding to the resonance condition $\Omega_1 = n\hbar\omega_r$. Inset: zoom of the current peak at $\Omega_1 = 2\hbar\omega_r$ for symmetric rates. The rest of the parameters (in units of ω_r) are: $t_1 = 0.2, g_1 = 0.008, \kappa = 5 \times 10^{-4}$.

strated experimentally in Ref. 55, as well as the physics of on-chip noise detection using two-level systems.^{45,52,56}

For large enough electron-boson coupling g_1 , additional resonances at $\Omega_1 \approx n\hbar\omega_r$ appear. An example for $n = 2$ is shown in the inset in figure 2a).

Note that the qubit-photon resonances are not present for the region $\epsilon_1 < 0$ since the photon mode is in its ground state at zero temperature and, hence, photon absorption inducing tunneling of the charge is not possible. As we shall discuss in the next subsection, this is no longer true in the presence of a second qubit that can induce excitations in the microwave resonator.

The corresponding Fano factor F_{11} , shown in figure 2b), exhibits a dip around $\epsilon_1 = 0$. There, interdot tunneling delocalizes the charge which, combined with the strong Coulomb blockade, reduces the noise and gives sub-Poissonian Fano factor, $F_{11} < 1$.^{46,57} As the level detuning ϵ_1 increases, the charge becomes localized, say in the left dot for $\epsilon_1 > 0$, and hence Poissonian noise from a single barrier (the one parametrized by Γ_L) is obtained.

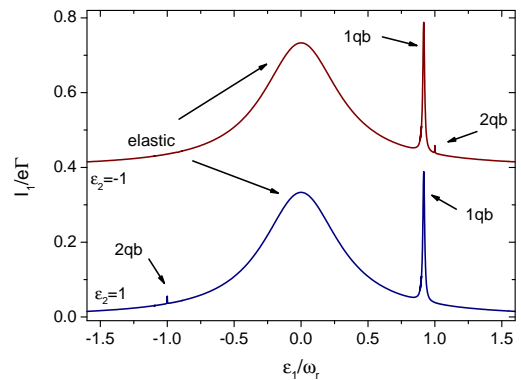


FIG. 3: (Color online) Steady state current in the first DQD as a function of its level position ϵ_1 for two different configurations of the second qubit: $\epsilon_2 = -1$ and $\epsilon_2 = 1$. The two examples have been vertically shifted (with an offset of 0.4) for the sake of clarity. Parameters (in units of ω_r): $g_1 = g_2 = g = 0.008, t_1 = t_2 = t = 0.2, \Gamma = 10^{-3}$ and $\kappa = 10^{-3}$.

This is so until the resonance conditions $\Omega_1 = n\hbar\omega_r$ are reached, where the noise is reduced again yielding $F_{11} < 1$. This sub-Poissonian value at resonance with the photon cavity reveals that the charge is transferred across the DQD with the simultaneous excitation of the resonator. The same kind of result is obtained for emission into a full bath of bosons.⁴⁶

Note also the small resonant feature in the region $\epsilon_1 < 0$. Even though in this configuration the extra charge is mainly localized in the left dot, there is a small probability of populating the right dot (and subsequently tunnel out from the right barrier). From the point of view of the qubit, this means that there is a small probability of populating the excited state and hence to emit photons. This can be easily seen if we write the qubit-photon interaction in the qubit eigenbasis $|e\rangle = \cos\frac{\theta}{2}|L\rangle + \sin\frac{\theta}{2}|R\rangle$ and $|g\rangle = \sin\frac{\theta}{2}|L\rangle - \cos\frac{\theta}{2}|R\rangle$, with $\theta = \arctan(\frac{2t_1}{\epsilon_1})$ being the angle that characterizes mixing in the charge subspace: $H_{e-res} = g_1(\cos\theta\tau_z + \sin\theta\tau_x)(a^\dagger + a)$, with $\tau_z = |e\rangle\langle e| - |g\rangle\langle g|$ and $\tau_x = |e\rangle\langle g| + |g\rangle\langle e|$. We have checked that photon emission at $\epsilon_1 \approx -1$ is small but finite (the photon occupation has a resonance around this detuning and increases from zero to $\langle n \rangle \approx 10^{-3}$, not shown), as a result of $|e\rangle \rightarrow |g\rangle$ relaxation processes. Dynamically, these rare events, where the qubit is excited for negative detuning such that photon emission is possible, contribute to the noise which shows a feature at $\Omega_1 = \omega_r$ with $\epsilon_1 < 0$. On the contrary, they do not change significantly the average current, demonstrating the superior sensitivity that noise has.

The effect on the transport properties of asymmetric tunneling rates is also shown in figure 2, where we considered that $\Gamma_{L,1} > \Gamma_{R,1}$. The current, figure 2a), exhibits the same qualitative behavior than the case with equal rates, with an elastic peak around $\epsilon = 0$ and satellite

peaks at the resonances qubit-resonator. On the contrary, the Fano factor changes completely for asymmetric rates, figure 2b). In this case, F_{11} presents a double peak structure in the region $\varepsilon = 0$, with the maximum of the peaks corresponding to super-Poissonian noise. This well-known effect can be understood from the analytical expression of the Fano factor⁵⁸ and, in particular, is originated from the smaller coupling to the drain reservoir which, ultimately, makes the Coulomb interaction more effective and gives rise to bunching in transport with $F_{11} > 1$. The same kind of bunching behavior is observed for the Fano factor at the qubit-photon resonances. It is interesting to compare this $F_{11} > 1$ at the one photon resonance with the result for a full bosonic bath which always results in sub-Poissonian noise.^{46,59} Hence super-Poissonian noise results from the qubit-photon coherent interaction. This result is also along the lines of Ref. 59, where the authors demonstrate that the bunching effect cannot be obtained from a picture without qubit coherences. In the context of lasing, this sort of super-Poissonian noise has been related to squeezing of the resonator state.⁶⁰

B. Two DQDs coupled to the transmission line resonator

We turn now to our original model in which two DQDs are coupled to the same photon mode of the microwave resonator, but uncoupled to each other. For simplicity, we consider first the same intra-dot tunnel couplings $t_i = t$ and equal electron-photon coupling $g_i = g$. It is assumed that the tunneling rates to left and right reservoirs are equal and also equivalent for both DQDs i.e., $\Gamma_{L,i} = \Gamma_{R,i} = \Gamma$, unless otherwise stated. As in the case for a single DQD, all the parameters are given in terms

of the bare frequency of the microwave resonator ω_r .

Results for the mean value of the stationary current passing through the first DQD, I_1 , as function of its level detuning ε_1 , while keeping the second DQD in a fixed level structure, are presented in figure 3. Similarly to the case for a single DQD, there is an elastic peak in I_1 around $\varepsilon_1 = 0$. A second, inelastic peak appears in the region where this qubit enters in resonance with the photon, $\Omega_1 \approx \hbar\omega_r$ revealing that this effect is entirely due to the coupling of this DQD with the resonator and thus will appear irrespective of the presence of the second DQD. We refer to this feature as the *one-qubit (1qb) peak*.

Interestingly, an additional peak in I_1 is observed in the emission part $\varepsilon_1 > 0$ for the case $\varepsilon_2 = -1$, and in the absorption part $\varepsilon_1 < 0$ with $\varepsilon_2 = 1$. The third peak arises when both DQDs are brought in resonance with each other, $\Omega_1 = \Omega_2$, with opposite detuning, $\varepsilon_1 = -\varepsilon_2$, but slightly out of resonance with the photon mode, $\Omega_1 = \Omega_2 \neq \hbar\omega_r$. It is a result of an indirect qubit-qubit interaction induced by the common coupling to the microwave resonator and therefore we refer to it as the *two-qubits (2qb) peak*. The fact that this resonance appears at an energy larger than the bare frequency ω_r reveals that the effective interaction is obtained via virtual photons: when both qubits are in resonance, the excitation in one of the DQDs is transferred to the other by virtually becoming a photon in the microwave resonator. Similar physics has been demonstrated experimentally in circuit-QED systems with superconducting qubits, see Ref. 61.

In order to have a better understanding of the induced qubit-qubit interaction, we derive an effective Hamiltonian for the regime where the 2qb-features appear, $\Omega_i - \omega_r > g$. Starting from the Hamiltonian $H_0 = H_{el} + H_{int} + H_{res} + H_{e-res}$, and restricting ourselves to states with $n = 0, 1$, we obtain to second order in the qubit-photon coupling:

$$H_{eff} = \sum_i \left(\frac{1}{2} \varepsilon_i \sigma_z^i + t_{i,eff} \sigma_x^i \right) + J_z \sigma_z^1 \sigma_z^2 - \sum_{i \neq j} J_{xz,ij} \sigma_z^i \sigma_x^j + \sum_i \frac{g_i^2}{\Omega_i^2} \left[t_i^2 \left(\frac{1}{\Omega_i - \omega_r} - \frac{1}{\Omega_i + \omega_r} \right) - \frac{\varepsilon_i^2}{\omega_r} \right]. \quad (7)$$

The effective Hamiltonian of equation (7) explicitly shows that the interaction of the qubits with a common photon mode translates into a shift of their frequencies, through the renormalized tunneling amplitude $t_i \rightarrow t_{i,eff} = t_i \left[1 + \frac{g_i^2}{\Omega_i} \left(\frac{1}{\Omega_i - \omega_r} - \frac{1}{\Omega_i + \omega_r} \right) \right]$, as well as two types of qubit-qubit interaction. The first one is Ising like with effective exchange constant $J_z = \sum_i \frac{g_1 g_2}{\Omega_i^2} \left[2t_i^2 \left(\frac{1}{\Omega_i - \omega_r} - \frac{1}{\Omega_i + \omega_r} \right) - \frac{\varepsilon_i^2}{\omega_r} \right]$, whereas the second one is an XZ exchange interaction with a coupling

strength $J_{xz,ij} = \frac{g_i g_j \varepsilon_j t_j}{\Omega_j^2} \left(\frac{1}{\Omega_j - \omega_r} - \frac{1}{\Omega_j + \omega_r} - \frac{2}{\omega_r} \right)$, where the presence of an electron in one qubit induces a transition in the other.

Neglecting the terms of order $1/\omega_r$ and $1/(\Omega_i + \omega_r)$ the effective Hamiltonian reads (the last, constant, term in

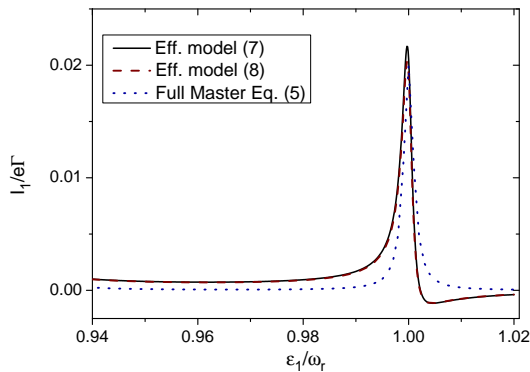


FIG. 4: (Color online) Comparison of the results for the steady state current in the first DQD as a function of its level position ε_1 , obtained with the full Master Equation (5) and with the models described by the effective Hamiltonians (7) and (8). Parameters: $\varepsilon_2 = -1$, $g_1 = g_2 = g = 0.008$, $t_1 = t_2 = t = 0.2$, $\Gamma = 10^{-3}$ and $\kappa = 10^{-3}$.

the hamiltonian is dropped):

$$H_{eff} = \sum_i \left(\frac{1}{2} \varepsilon_i \sigma_z^i + t'_{i,eff} \sigma_x^i \right) + J'_z \sigma_z^1 \sigma_z^2 - \sum_{i \neq j} J'_{xz,ij} \sigma_z^i \sigma_x^j. \quad (8)$$

The effective coupling constants

$$\begin{aligned} t'_{i,eff} &= t_i \left[1 + \frac{g_i^2}{\Omega_i} \left(\frac{1}{\Omega_i - \omega_r} \right) \right] \\ J'_z &= \sum_i \frac{2g_1 g_2 t_i^2}{\Omega_i^2 (\Omega_i - \omega_r)} \\ J'_{xz,ij} &= \frac{g_i g_j \varepsilon_j t_j}{\Omega_j^2} \left(\frac{1}{\Omega_j - \omega_r} \right), \end{aligned} \quad (9)$$

show dispersive shifts due to the off-resonant interaction with the microwave resonator photons.⁶²

The interaction terms in equation (8) capture quite well the 2qb transport resonance. This is explicitly shown in figure 4 where we plot a comparison of the current calculated with an effective master equation obtained from the models (7) and (8) against the one obtained with the full master equation given by (5), around the resonance $\Omega_1 \sim \Omega_2$. It can be noticed that the effective models reproduce the width and height of the 2qb peak. Of course, outside this resonance the effective model fails and cannot describe transport in the full regime of level detunings.

Once we have shown that the 2qb feature comes indeed from a resonator-induced interaction between both charge qubits, we describe how the non-local character of this interaction can be easily explored.

This is explicitly demonstrated in figure 5 where we show results for I_1 as a function of ε_1 around the two-qubit resonance condition and for different values of ε_2 .

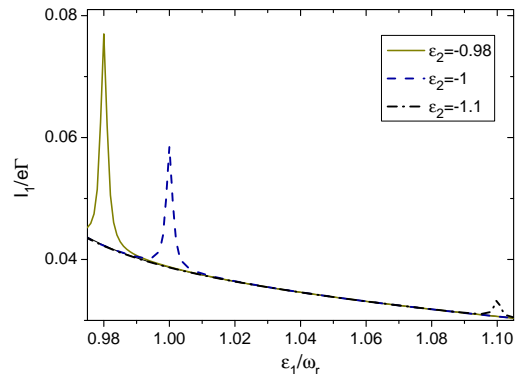


FIG. 5: (Color online) Current on the first DQD as a function of ε_1 around the qubit-qubit resonance, for different values of ε_2 . Rest of the parameters as those used in Fig. 3.

The 2qb-peak in the current through one qubit clearly moves as one varies the level position in the other, while the 1qb resonance remains unaltered (not shown) upon changing ε_2 . We can also note that as the difference $|\Omega_i - \omega_r|$ increases, the effective couplings given by equation (9) decrease and therefore the induced qubit-qubit interaction is turned off. Experiments along these lines have been recently reported for transport through single carbon-nanotube quantum dots, where non-local control mediated by a photon cavity (in the classical limit) has been demonstrated.⁶³ Thus we expect that an experimental test of our prediction in figure 5 is within reach.

An even more interesting possibility is to non-locally manipulate the qubit-qubit induced interaction by tuning the *dissipative* coupling of one of the qubits with its fermionic reservoirs. For example, a strong coupling to the right reservoir in, say, qubit 2 induces a transport version of the quantum Zeno effect which tends to freeze the dynamics of the second qubit by effectively localizing the charge in the left dot of the DQD2, with $\langle \sigma_z^2 \rangle \rightarrow 1$. We demonstrate this effect in figure 6 where the current through the first DQD as a function of $\Gamma_{R,2}$ is shown for the two-qubit resonance condition $\varepsilon_1 = -\varepsilon_2$, with $\Gamma_{\beta,1} = \Gamma_{L,2} = \Gamma$. It is observed there that for fixed qubits parameters, the current through DQD1 is strongly reduced by increasing merely the rate $\Gamma_{R,2}$ of the second DQD. We can reinforce the interpretation of this results by recalling the effective qubit-qubit interaction: for very large $\Gamma_{R,2}$ one can replace the operators of the second qubit by the corresponding mean value; then the effective coupling constants for the first qubit are also frozen and results in a smaller effective coupling.

To check more critically the presence of non-local correlations mediated by the cavity, we study how nontrivial noise correlations develop. The Fano factor for the DQD1 shows the same qualitative behavior exhibited in the single-qubit case (for symmetric rates with the reservoirs), with sub-Poissonian regions around all resonances of the problem, see figure 7.

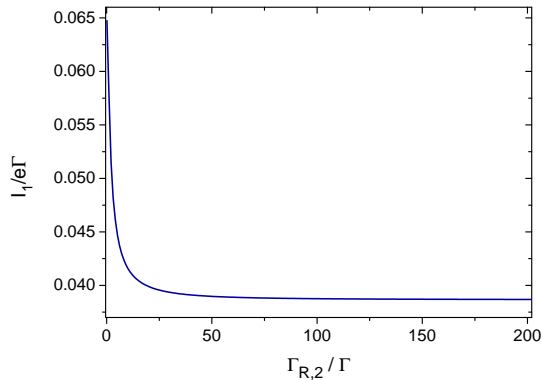


FIG. 6: (Color online) Current on the first DQD as a function of $\Gamma_{R,2}$ for the resonance $\varepsilon_1 = -\varepsilon_2 = 1$. Rest of the parameters (in units of ω_r): $t = 0.2$, $\Gamma_{L,1} = \Gamma_{R,1} = \Gamma_{L,2} = 10^{-3}$, $\kappa = 10^{-3}$.

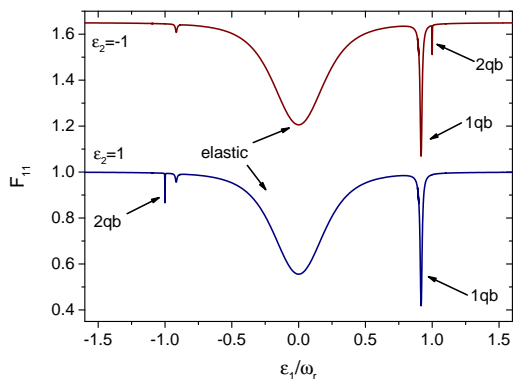


FIG. 7: (Color online) Fano factor for the first DQD as a function of the level position ε_1 for two different configurations of the second qubit: $\varepsilon_2 = -1$ and $\varepsilon_2 = 1$. The results are vertically shifted (offset of 0.65) for the sake of clarity. Rest of the parameters as in Fig. 3.

More crucially, the cross-correlations between separate currents through both DQDs, F_{12} , develop sharp resonances at the qubit-qubit resonance $\Omega_1 = \Omega_2$ (figure 8). Apart from these clear resonances, other small features signal finite microwave resonator occupations which lead to non-zero correlations. As the coupling with the resonator increases, such features, and more generally the overall behavior as a function of level detuning, can become rather intricate. Figure 9 shows the cross-correlations for increasing g in the region around the 2qb resonance. This figure reveals that the peak emerged around this resonance splits as the qubits-resonator coupling becomes larger. At the same time, the resonances become broader such that the function $F_{12}(\varepsilon_1, g)$ develops a two-lobe structure. As we shall show in the next Section, this characteristic structure signals the formation of Bell states between both qubits and hence the development of non-local entanglement.

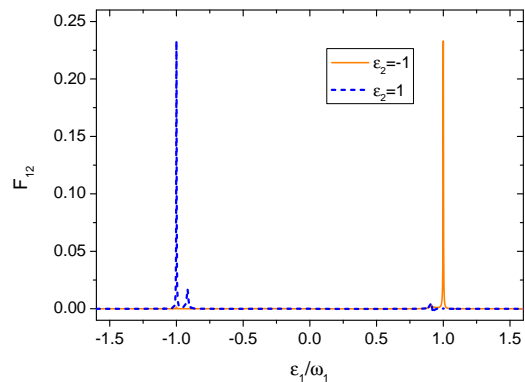


FIG. 8: (Color online) Correlators for the current passing through both qubits F_{21} , for $\varepsilon_2 = -1$ and $\varepsilon_2 = 1$. Same parameters as in Fig.3.

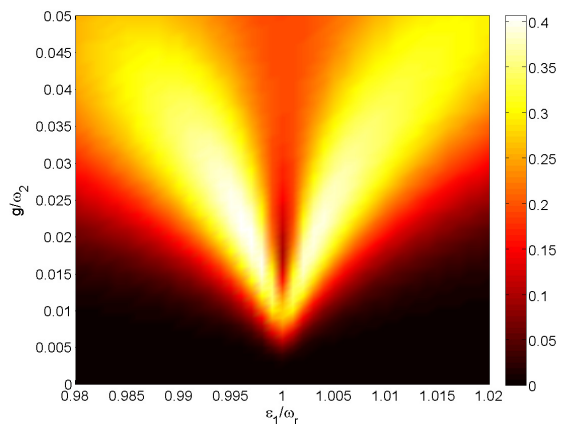


FIG. 9: (Color online) Colormap of the cross-correlations F_{12} around the two-qubit resonance as a function of the level detuning ε_1 and the coupling parameter with the resonator, g . Rest of the parameters (in units of ω_r): $\varepsilon_2 = -1$, $t = 0.2$, $\Gamma = 10^{-3}$, $\kappa = 10^{-3}$.

IV. QUBIT-QUBIT ENTANGLEMENT

So far we have demonstrated that transport exhibits signatures of the induced interaction between the DQDs due to the common coupling to photons in the microwave resonator. Here, we go a step further and explicitly demonstrate that this common coupling can generate entanglement. In particular, we show that qubit-qubit entanglement under *nonequilibrium* conditions can be generated by virtual photons. For quantifying the nonequilibrium entanglement we make use of the Concurrence,⁶⁴ a measure of entanglement which arises from the entanglement of formation and that is calculated by means of the density matrix of the system in the computational basis. We calculate the Concurrence of the steady state $\hat{P}\rho^{stat}$, which corresponds to the projection of the stationary density matrix onto the two-qubits subspace with a proper normalization,⁴⁷ and trace out the states of the

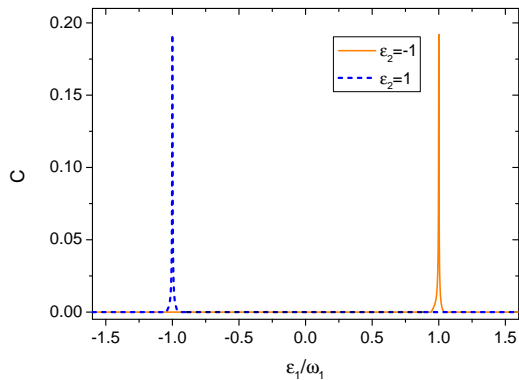


FIG. 10: (Color online) Concurrence for $\varepsilon_2 = -1$ and $\varepsilon_2 = 1$. Rest of the parameters as in Fig.3.

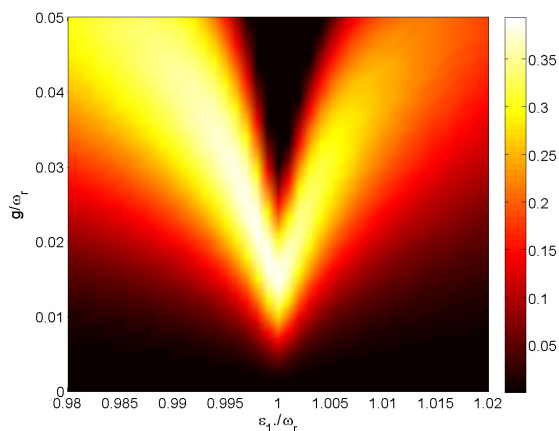


FIG. 11: (Color online) Colormap of the Concurrence around the two-qubit resonance as a function of the level detuning ε_1 and the coupling parameter with the resonator, g . Rest of the parameters (in units of ω_r): $\varepsilon_2 = -1$, $t = 0.2$, $\Gamma = 10^{-3}$, $\kappa = 10^{-3}$.

bosonic mode.

Numerical results for the Concurrence, C , considering the same interdot tunneling amplitude in both qubits, $t_i = t$, and symmetric electron-photon coupling $g_i = g$ are shown in figure 10 for two different level detunings in the second qubit. For the typical value of the coupling $g = 0.008$ used here, C shows sharp features in the 2qb resonance, $\varepsilon_1 = -\varepsilon_2$.

In figure 11 we show the detail of Concurrence in the region of the 2qb resonance, as a function of ε_1 and the coupling strength to the microwave resonator g , for $\varepsilon_2 = -1$. Here we find that, in the same way as the cross-correlators F_{12} (figure 9), the peak exhibited by the Concurrence around resonance splits and develops a two-lobe structure as the coupling g becomes larger. The similarity between these two quantities shows that current cross-correlations in the above configuration constitute an indicator of non-local qubit-qubit entanglement.

The previous interpretation is supported by an analy-

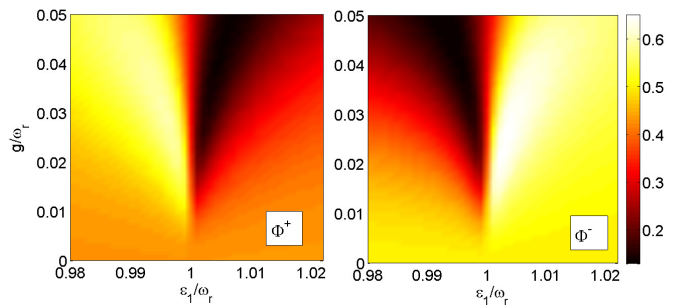


FIG. 12: (Color online) Stationary occupation probability of the Bell state $|\phi^+\rangle$ (left) and $|\phi^-\rangle$ (right) around the two-qubit resonance. Same axes and parameters as in Fig. 11.

sis of the steady state populations of the system. If the analysis is done in terms of the populations in the local basis (e.g. $|\alpha_1, \alpha_2\rangle$, with $\alpha = L, R$) the double-peaked structure of Figs. 11 and 9 is hard to explain, since all local populations exhibit just a single peak around resonance. However, considering the stationary populations in the Bell basis of maximally entangled states, a different picture arises. Figure 12 shows the population of the Bell states $|\Phi^\pm\rangle$,⁶⁵ which written in terms of the occupation of the L/R dots of each DQD read:

$$|\Phi^\pm\rangle = \frac{1}{\sqrt{2}} (|R_1, R_2\rangle \pm |L_1, L_2\rangle). \quad (10)$$

The occupation probability of these two states show a double peak structure as g becomes larger. Importantly, these peaks occur asymmetrically such that each Bell state has maximum occupation on either side of the resonance. The two-lobe structure of both the Concurrence and the cross-correlations thus correspond to the two maxima of the $|\Phi^\pm\rangle$ Bell state populations. The remaining Bell states

$$|\Psi^\pm\rangle = \frac{1}{\sqrt{2}} (|R_1, L_2\rangle \pm |L_1, R_2\rangle) \quad (11)$$

just show single peaks centered on resonance and presumably do not greatly contribute to the overall form of the current cross-correlations.

V. ASYMMETRIC COUPLING TO THE MICROWAVE RESONATOR, $g_1 \neq g_2$.

Finally, we also explore the effect of asymmetric values of the electron-photon coupling strengths for each qubit, $g_1 \neq g_2$. Experimentally, this asymmetry can be achieved by changing both the capacitive coupling of each DQD to the microwave resonator C_i^c as well as the capacitance of each DQD to ground C_i^g , as the couplings scale as $g_i \sim \frac{C_i^c}{C_i^c + C_i^g}$.⁸ Our motivation here is to explore the possibility of detecting the interaction-induced shifts directly in transport. Further motivation comes from Ref.

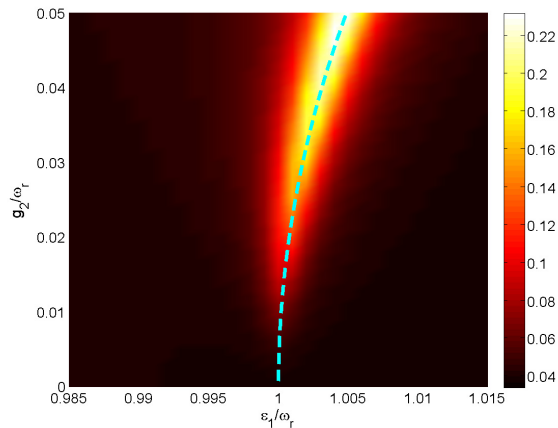


FIG. 13: (Color online) Colormap of the current around the qubit-qubit resonance condition as a function of the level detuning ε_1 and the coupling parameter with the resonator for the second qubit, g_2 , for fixed $g_1 = 0.008$. The dashed line indicate the values of ε_1 corresponding to the renormalized frequency of the first qubit $\Omega_{1,eff} = \Omega_{2,eff}$ predicted by the effective Hamiltonian (8). Rest of the parameters: $\varepsilon_2 = -1$, $t = 0.2$, $\Gamma = 10^{-3}$, $\kappa = 10^{-3}$.

66, which theoretically proposed the use of inhomogeneous coupling between two-level systems and a single quantized mode to generate and control multipartite entangled states

The current as function of ε_1 and g_2 is shown in figure 13 for the region around $\varepsilon_1 \approx -\varepsilon_2$. For increasing g_2 , the position of the resonance is shifted with respect to the initial value for $g_1 = g_2$. As expected, this can be understood by means of the renormalization of the intra-dot tunneling coupling $t_{i,eff}$ in the effective Hamiltonian of equation (8). This renormalization leads in turn to a change in the frequency of the qubits as $\Omega_{i,eff} = \sqrt{\varepsilon_i^2 + 4t_{i,eff}^2}$. Therefore, the current shows a dispersive shift at values of ε_1 accordingly to the new, effective qubit-qubit resonance condition given by $\Omega_{1,eff} = \Omega_{2,eff}$. The dispersive shift obtained with the full numerics agrees with the one given by the effective Hamiltonian, represented by the dashed line in figure 13. Measurements along these lines would constitute further proof of resonator-induced interaction between qubits. The same dispersive shift is also observed in the shot noise cross-correlations, figure 14a), where again, the 2qb resonance in F_{12} splits for large enough coupling.

Finally we present the same analysis for the Concurrence in figure 14b). Apart from the shift, we can notice that, in general, the Concurrence has larger values in comparison to the case with $g_1 = g_2$, indicating that the asymmetry between the coupling parameters of each qubit with the bosonic mode makes the qubit-qubit entanglement to be more robust.

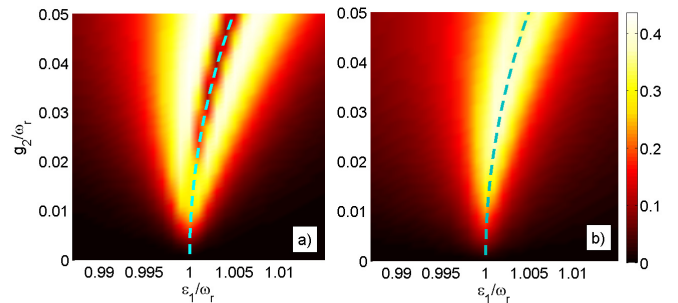


FIG. 14: (Color online) Colormap of a) cross-correlations F_{12} and b) Concurrence as a function of ε_1 and g_2 , for fixed $g_1 = 0.008$, and around the two-qubit resonance. The dashed line indicate the renormalized two-qubit resonance $\Omega_{1,eff} = \Omega_{2,eff}$. Rest of the parameters as in Fig. 13

VI. CONCLUSION

We studied theoretically photon-mediated transport and the generation of steady state correlations between two open charge qubits defined in spatially-separated double quantum dots which are coupled to a common transmission line resonator. Our results demonstrate that the qubits are entangled due to the indirect coupling induced by photons in the microwave resonator. Considering that each qubit is open to electronic reservoirs, we have analyzed their transport properties and found that they reveal the qubit-qubit interaction. In particular, we calculated the zero-frequency shot noise and the current cross-correlations as a function of the level detuning of one of the qubits, and observed the presence of different resonant features in the regions where the qubit enters in resonance with the photon as well as with the other qubit. In the examples we studied here, the quantum correlations involved in the transport of charge and which are responsible of the signal in the cross-correlations, yield in a finite value for the Concurrence when the qubits interact due to off-resonant photons. Therefore, we propose that measurements of current correlations could be used as a possible method for detecting entanglement and, in general, qubit-qubit interactions mediated by the microwave resonator. This proposal is motivated also in the context of recent experimental achievements demonstrating the coupling of semiconductor QDs to microwave resonators.^{14–17,67}

The model presented here constitute a step further in the study of this kind of hybrid systems, which can be relatively easily extended to several qubits. In general, this system let us to explore the interplay between coherent interactions, entanglement and the effect of dissipation and noise. Moreover, our model can also be applied to charge qubits defined by Cooper-pair boxes or to systems in which the quantum dots are coupled to a nanoelectromechanical resonator.

Note added: While finishing this manuscript, two theoretical works analyzing a similar setup to ours have appeared. The first work⁶⁸ focuses on the effect that non-

local interaction between two DQDs resonantly coupled to the oscillator has on finite bias voltage transport properties (which are prone to finite temperature effects in the electronic reservoirs). In contrast, we here focus on a different operating regime where the non-local interaction is induced off-resonance and transport occurs at very large voltages. In this large-voltage regime, the results are essentially independent on the electronic reservoir temperature and are valid at arbitrary couplings to the reservoirs. This large voltage regime is also analyzed in the second work,⁶⁹ where some overlapping results about photon-mediated transport and finite shot noise cross-correlations have been reported.

Acknowledgments

We are grateful to N. Lambert, F. Nori and P. Samuelsson for interesting discussions and for letting us know about their works^{68,69} previous to submission to the arXiv. We would like to thank T. Kontos for helpful comments. This work was supported by the European Commission (STREP PICC), the Alexander von Humboldt Foundation, the DAAD and DFG Grants BR 1528/7-1, 1528/8- 1, SFB 910, and GRK 1558 and the Spanish MINECO through grants FIS2009-08744 and FIS2012-33521.

-
- ¹ A. Wallraff, D. I. Schuster, A. Blais, L. Frunzio, R.-S. Huang, J. Majer, S. Kumar, S. M. Girvin, and R. J. Schoelkopf, *Nature (London)* **431**, 162 (2004).
 - ² A. Blais, R.-S. Huang, A. Wallraff, S. M. Girvin, and R. J. Schoelkopf, *Phys. Rev. A* **69**, 062320 (2004).
 - ³ J. Q. You and F. Nori, *Phys. Today* **58**, 42 (2005).
 - ⁴ R. J. Schoelkopf and S. M. Girvin, *Nature (London)* **451**, 664 (2008).
 - ⁵ J. Q. You and F. Nori, *Nature (London)* **474**, 589 (2011).
 - ⁶ T. Niemczyk, F. Deppe, H. Huebl, E. P. Menzel, F. Hocke, M. J. Schwarz, J. J. Garcia-Ripoll, D. Zueco, T. Hümmer, E. Solano, et al., *Nature Phys.* **6**, 772 (2010).
 - ⁷ Z.-L. Xiang, S. Ashhab, and F. Nori, *Rev. Mod. Phys.* **85**, 623 (2013).
 - ⁸ S. Childress, A. S. Sørensen, and M. D. Lukin, *Phys. Rev. A* **69**, 042302 (2004).
 - ⁹ M. Trif, V. N. Golovach, and D. Loss, *Phys. Rev. B* **77**, 045434 (2008).
 - ¹⁰ A. Cottet and T. Kontos, *Phys. Rev. Lett.* **105**, 160502 (2010).
 - ¹¹ X. Hu, Y.-x. Liu, and F. Nori, *Phys. Rev. B* **86**, 035314 (2012).
 - ¹² P.-Q. Jin, M. Marthaler, A. Shnirman, and G. Schön, *Phys. Rev. Lett.* **108**, 1905 (2012).
 - ¹³ K. D. Petersson, L. W. McFaul, M. D. Schroer, M. Jung, J. M. Taylor, A. A. Houck, and J. R. Petta, *Nature (London)* **490**, 380 (2012).
 - ¹⁴ M. R. Delbecq, V. Schmitt, F. Parmentier, N. Roch, J. Vienne, G. Fève, B. Huard, C. Mora, A. Cottet, and T. Kontos, *Phys. Rev. Lett.* **107**, 256804 (2011).
 - ¹⁵ T. Frey, P. J. Leek, M. Beck, A. Blais, T. Ihn, K. Ensslin, and A. Wallraff, *Phys. Rev. Lett.* **108**, 046807 (2012).
 - ¹⁶ T. Frey, P. J. Leek, M. Beck, J. Faist, A. Wallraff, K. Ensslin, T. Ihn, and M. Büttiker, *Phys. Rev. B* **86**, 115303 (2012).
 - ¹⁷ H. Toida, T. Nakajima, and S. Komiyama, *Phys. Rev. Lett.* **110**, 066802 (2013).
 - ¹⁸ S. Ashhab, J. R. Johansson, A. M. Zagoskin, and F. Nori, *New J. Phys.* **11**, 023030 (2009).
 - ¹⁹ P.-Q. Jin, M. Marthaler, J. H. Cole, A. Shnirman, and G. Schön, *Phys. Rev. B* **84**, 035322 (2011).
 - ²⁰ R. Okuyama, M. Eto, and T. Brandes, *J. Phys. Soc. Jpn.* **82**, 013704 (2013).
 - ²¹ C. Xu and M. G. Vavilov, Preprint arXiv:1303.6965.
 - ²² W. G. van der Wiel, S. de Franceschi, J. M. Elzerman, T. Fujisawa, S. Tarucha, and L. P. Kouwenhoven, *Rev. Mod. Phys.* **75**, 1283 (2003).
 - ²³ N. Lambert, Y.-n. Chen, R. Johansson, and F. Nori, *Phys. Rev. B* **80**, 165308 (2009).
 - ²⁴ T. Vorrath and T. Brandes, *Phys. Rev. B* **68**, 035309 (2003); L. D. Contreras-Pulido and R. Aguado, *Phys. Rev. B* **77**, 155420 (2008).
 - ²⁵ K. Blum, *Density Matrix Theory and Applications* (Plenum Press, NY, 1981).
 - ²⁶ H. P. Breuer and F. Petruccione, *The Theory of open quantum systems* (Oxford University Press, UK, 2002).
 - ²⁷ T. H. Stoof and Y. V. Nazarov, *Phys. Rev. B* **53**, 1050 (1996).
 - ²⁸ T. Brandes, *Phys. Rep.* **408**, 315 (2005).
 - ²⁹ D. F. Walls and G. J. Milburn, *Quantum Optics* (Springer-Verlag, Berlin, 2008).
 - ³⁰ E. Casanova, G. Romero, I. Lizuain, J. García-Ripoll, and E. Solano, *Phys. Rev. Lett.* **105**, 263603 (2010).
 - ³¹ D. Marcos, C. Emary, T. Brandes and R. Aguado, *Phys. Rev. B* **83**, 125426 (2011); C. Emary and R. Aguado, *Phys. Rev. B* **84**, 085425 (2011).
 - ³² G. Burkard, D. Loss, and E. V. Sukhorukov, *Phys. Rev. B* **61**, R16303 (2000).
 - ³³ G. B. Lesovik, T. Martin, and G. Blatter, *Eur. Phys. J. B* **24**, 287 (2001).
 - ³⁴ F. Plastina, R. Fazio, and G. M. Palma, *Phys. Rev. B* **64**, 113306 (2001).
 - ³⁵ N. M. Chtchelkatchev, G. Blatter, G. B. Lesovik, and T. Martin, *Phys. Rev. B* **66**, 161320(R) (2002).
 - ³⁶ C. W. J. Beenakker, C. Emary, M. Kindermann, and J. L. van Velsen, *Phys. Rev. Lett.* **91**, 147901 (2003).
 - ³⁷ P. Samuelsson, E. V. Sukhorukov, and M. Büttiker, *Phys. Rev. Lett.* **91**, 157002 (2003).
 - ³⁸ C. Emary, *Phys. Rev. B* **80**, 161309(R) (2009).
 - ³⁹ A. Bednorz and W. Belzig, *Phys. Rev. B* **83**, 125304 (2011).
 - ⁴⁰ C. Flindt, T. Novotný, and A.-P. Jauho, *Phys. Rev. B* **70**, 205334 (2004).
 - ⁴¹ N. Lambert, R. Aguado, and T. Brandes, *Phys. Rev. B* **75**, 045340 (2007).
 - ⁴² C. Emary, *Phys. Rev. B* **80**, 235306 (2009).
 - ⁴³ For the relation between (anti)bunching and the Fano factor in electronic transport, also cf. C. Emary *et al.*, *Phys. Rev. B* **85**, 165417 (2012).
 - ⁴⁴ T. Brandes and B. Kramer, *Phys. Rev. Lett.* **83**, 3021

- (1999).
- ⁴⁵ R. Aguado and L. P. Kouwenhoven, Phys. Rev. Lett. **84**, 1986 (2000).
- ⁴⁶ R. Aguado and T. Brandes, Phys. Rev. Lett. **92**, 206601 (2004).
- ⁴⁷ T. Brandes and N. Lambert, Phys. Rev. B **67**, 125323 (2003).
- ⁴⁸ B. Dong, H. L. Cui, X. L. Lei, and N. J. M. Horing, Phys. Rev. B **71**, 045331 (2005).
- ⁴⁹ N. Lambert and F. Nori, Phys. Rev. B **78**, 214302 (2008).
- ⁵⁰ T. J. Harvey, D. A. Rodrigues, and A. D. Armour, Phys. Rev. B **78**, 024513 (2008).
- ⁵¹ V. Koerting, T. L. Schmidt, C. B. Doiron, B. Trauzettel, and C. Bruder, Phys. Rev. B **79**, 134511 (2009).
- ⁵² G. Granger, D. Taubert, C. E. Young, L. Gaudreau, A. Kam, S. A. Studenikin, P. Zawadzki, D. Harbusch, D. Schuh, W. Wegscheider, et al., Nature Phys. **8**, 522 (2012).
- ⁵³ Y. V. Nazarov, Phys. B **189**, 57 (1998).
- ⁵⁴ Note that the above transport configuration is essentially identical to the Josephson quasiparticle cycle of a superconducting single electron transistor with charging energy much larger than the Josephson coupling. Indeed, lasing in a Cooper pair box coupled to a superconducting resonator was experimentally demonstrated by Astafiev *et al.*, Nature (London) **449**, 588 (2007).
- ⁵⁵ T. Fujisawa, T. Oosterkamp, W. van der Wiel, B. Broer, R. Aguado, S. Tarucha, and L. Kouwenhoven, Science **282**, 932 (1998).
- ⁵⁶ V. S. Khrapai, S. Ludwig, J. P. Kotthaus, H. P. Tranitz, H. P. and W. Wegscheider, Phys. Rev. Lett. **97**, 176803 (2006); S. Gustavsson, M. Studer, R. Leturcq, T. Ihn, K. Ensslin, D. C. Driscoll and A. C. Gossard, Phys. Rev. Lett. **99**, 206804 (2007); Y.-F. Chen, D. Hover, S. Sendelbach, L. Maurer, S. T. Merkel, E. J. Pritchett, F. K. Wilhelm, and R. McDermott, Phys. Rev. Lett. **107**, 217401 (2011).
- ⁵⁷ M.-S. Choi, F. Plastina, and R. Fazio, Phys. Rev. B **67**, 045105 (2003).
- ⁵⁸ B. Elattari and S. A. Gurvitz, Phys. Lett. A **292**, 289 (2002).
- ⁵⁹ G. Kießlich, E. Schöll, T. Brandes, F. Hohls, and R. J. Haug, Phys. Rev. Lett. **99**, 206602 (2007).
- ⁶⁰ J. Jin, M. Marthaler, P.-Q. Jin, D. Golubev and G. Schön, Preprint arXiv:1210.5698.
- ⁶¹ J. Majer, J. M. Chow, J. M. Gambetta, J. Koch, B. R. Johnson, J. A. Schreier, L. Frunzio, D. I. Schuster, A. A. Houck, A. Wallraff, et al., Nature (London) **449**, 443 (2007).
- ⁶² Note that we have effectively removed the photons from the problem, this is the reason why the Hamiltonian is not in the standard dispersive form.,.
- ⁶³ M. R. Delbecq, L. E. Bruhat, J. J. Viennot, S. Datta, A. Cottet, and T. Kontos, Nature Comm. **4**, 1400 (2013).
- ⁶⁴ S. Hill and W. K. Wootters, Phys. Rev. Lett. **78**, 5022 (1997); W. K. Wootters, Phys. Rev. Lett. **80**, 2245 (1998).
- ⁶⁵ S. Popescu and D. Rohrlich, in *Introduction to Quantum Computation and Information*, edited by H.-K Lo, S. Popescu and T. Spiller (World Scientific, Singapore, 1998).
- ⁶⁶ C. E. López, F. Lastra, G. Romero, E. Solano, and J. C. Retamal, Phys. Rev. A **85**, 032319 (2012).
- ⁶⁷ T. Frey, P. J. Leek, M. Beck, K. Ensslin, A. Wallraff, and T. Ihn, Appl. Phys. Lett. **98**, 262105 (2011).
- ⁶⁸ C. Bergenfeldt and P. Samuelsson, Preprint arXiv:1302.5640.
- ⁶⁹ N. Lambert, C. Flindt and F. Nori, Preprint arXiv:1303.7449.